Solid State Phenomena
ISSN: 1662-9779, Vol. 391, pp 65-77
doi:10.4028/p-vSvpd4

Submitted: 2026-01-16
Revised: 2026-02-16
Accepted: 2026-02-18
Online: 2026-04-20

Enabling the Reuse of Single-Lap Adhesive-Bonded Joints through Laser Cleaning and Texturing

Vincenzina Siciliani[1,a*], Matteo Benvenuto[2,b], Chiara Mandolfino[2,c], Barbara Reggiani[1,3,d] and Leonardo Orazi[1,4,e]

[1]DISMI – University of Modena and Reggio Emilia, via Amendola 2, 42122, Reggio Emilia, Italy

[2]DIME – University of Genoa, Via Opera Pia 15, 16145, Genoa, Italy

[3]INTERMECH – University of Modena and Reggio Emilia, Piazzale Europa 1, 42124, Reggio Emilia, Italy

[4]EN&TECH – University of Modena and Reggio Emilia, Piazzale Europa 1, 42124, Reggio Emilia, Italy

[a*]vincenzina.siciliani@unimore.it, [b]matteo.benvenuto@edu.unige.it, [c]chiara.mandolfino@unige.it, [d]barbara.reggiani@unimore.it, [e]leonardo.orazi@unimore.it

*corresponding author

Keywords: laser ablation, bonding joint, rebonding.

Abstract. Adhesive bonding is widely employed for joining complex-shaped components due to its ability to distribute stresses uniformly, preserve material integrity, and eliminate mechanical fasteners. However, the permanent nature of conventional adhesives and the difficulty of clean disassembly hinder the reuse of bonded joints, limiting recyclability and sustainability. This study investigates laser cleaning as an enabling technology for re-bonding single-lap joints. An ultrashort pulsed laser was applied to remove residual epoxy adhesive from AA6061 aluminum alloy substrates after debonding. Surface characterization revealed that laser ablation produces micrometric roughness, and laser processing can be further tailored to generate laser-induced periodic surface structures (LIPSS), influencing morphology, chemistry, and wettability. Mechanical testing demonstrated that laser cleaning also improves the tensile lap-shear strength of re-bonded untreated joints. These findings confirm that laser cleaning effectively restores substrate surfaces and, when combined with controlled texturing, can enhance bonding performance. The proposed approach supports repair and recycling strategies, contributing to extended component lifecycles and circular economy objectives.

Introduction

Adhesive bonding has become a key joining technology in modern engineering, particularly in sectors such as aerospace, automotive, and transportation, where lightweight structures and complex geometries are essential. Unlike traditional mechanical fastening or welding, adhesive bonding offers several advantages: it enables uniform stress distribution, reduces stress concentrations, preserves the integrity of the base material, and eliminates the need for additional components such as rivets or mechanical fasteners [1–4]. Furthermore, adhesive joints contribute to weight reduction, vibration damping, and corrosion resistance, making them highly attractive for structural applications [5]. Among the various materials used in these industries, aluminum alloys stand out due to their high strength-to-weight ratio, corrosion resistance, and excellent machinability. Alloys such as AA6xxx and AA7xxx series are widely employed in automotive body structures, aircraft components, and marine applications [6,7]. However, the performance of adhesive joints strongly depends on the surface condition of the adherends, which governs adhesion mechanisms at the interface [8].

Surface preparation is therefore a critical step in adhesive bonding. Conventional methods include mechanical abrasion (e.g., grit blasting, sanding) and chemical treatments (e.g., etching, anodizing), which aim to increase surface roughness, remove contaminants, and modify surface chemistry to enhance wettability [9–11]. While effective, these methods present drawbacks such as limited accuracy, environmental concerns, and difficulties in automating the process [12]. In this context, laser-based surface treatments have emerged as a promising alternative, offering high precision, flexibility, and environmental sustainability [13,14]. Laser texturing has been extensively investigated for its ability to create controlled micro and nano-scale features that increase the effective bonding area and promote mechanical interlocking [15–19]. Studies have shown that laser-induced grooves, dimples, and periodic structures can significantly improve lap-shear strength and shift failure modes from adhesive to cohesive [20–22]. Moreover, laser processing can simultaneously modify surface chemistry and wettability, further enhancing adhesion [23].

Despite these advances, the reuse of adhesive-bonded joints remains a major challenge for sustainable manufacturing. Conventional adhesives are generally considered permanent, and disassembly typically requires destructive methods such as mechanical cutting, thermal degradation, or chemical dissolution, which often damage the substrates and hinder their reuse [24]. This limitation conflicts with the principles of the circular economy, which aims to minimize waste and maximize resource efficiency by extending product lifecycles and enabling component recovery [25]. In high-value sectors such as aerospace and automotive, where aluminum components are costly and energy-intensive to produce, the inability to reuse bonded joints represents a significant environmental and economic burden. Therefore, developing technologies that allow clean disassembly and re-bonding is essential to reduce raw material consumption, lower greenhouse gas emissions, and comply with increasingly stringent sustainability regulations [26].

To address this issue, laser cleaning represents an innovative solution for post-debonding surface preparation. Laser cleaning employs a continuous or pulsed laser to ablate residual adhesive and contaminants: the pulsed laser has the major advantage of not damaging the underlying substrate [27,28]. Compared to abrasive or chemical cleaning, laser cleaning offers several advantages: it is a non-contact process, leaves no chemical residues, minimizes substrate alteration, and can be easily automated [29]. Furthermore, by adjusting process parameters, laser cleaning can generate micro-textures that improve wettability and create favorable conditions for re-bonding [30]. Recent studies have shown that the chemical effect of laser cleaning on aluminum alloys leads to increased mechanical performance compared to untreated surfaces [7,8]. For instance, Morello et al. [8] reported that laser cleaning alone increased the apparent shear strength of re-bonded AA6082 joints compared to untreated samples, while a combined approach of laser texturing followed by cleaning achieved even higher strength values. Similarly, Min et al. [7] highlighted that laser-induced modifications in morphology, chemistry, and wettability are key factors influencing adhesion performance.

These findings suggest that integrating laser cleaning, in the sense of ablating adhesive residues together with the chemical treatment produced by the laser, into the lifecycle of adhesive-bonded assemblies can significantly enhance repairability and recyclability, reducing waste and supporting sustainable manufacturing strategies. By enabling the reuse of bonded joints, laser cleaning contributes to resource efficiency and aligns with global efforts to reduce environmental impact in manufacturing. In particular, the use of lasers could perform the dual function of removing adhesive residues and pre-treating the surface for subsequent re-bonding.

The present work investigates the application of ultrashort pulse laser texturing and cleaning for enabling the reuse and improving the performance of single-lap adhesive-bonded joints made of Aluminum AA6061. The study compares two parallel methodologies. In the first case, three different pre-treatments are carried out on the substrates to increase the adhesive strength, followed by the adhesive bonding and the evaluation of the shear strength. The second methodology involves the pre-treatment of the surfaces, bonding the joints by adding a component to enable the controlled detachment, detaching the joints, and removing the residual epoxy adhesive after detachment. Finally, the joints are re-bonded, and the strength of the rebonding is evaluated. The resulting surface morphology is characterized to relate it to mechanical performances.

The goal is to assess the feasibility of laser texturing and cleaning as a robust and environmentally friendly method for extending the service life of adhesive-bonded structures and advancing circular economy principles in structural joining technologies.

Materials and Methods

Substrates and adhesive used.

The single-lap joint specimens were prepared in accordance with ASTM D1002 [31], which defines the geometry and the procedures for preparing specimens for shear strength tests of adhesive joints. In particular, the standard specifies the use of substrates with dimensions of 100 × 25 × 1.6 mm, overlapped with a length of 12.5 mm. The substrates were made of 6061-T6 aluminum alloy, an Al-Mg-Si alloy widely used in structural applications due to its favorable combination of mechanical strength, light weight, corrosion resistance, and workability. The substrates were bonded using a thixotropic two-component structural epoxy adhesive (3M™ EPX DP490), characterized by high mechanical strength, good toughness, and the ability to maintain a controlled adhesive layer thickness during assembly. Thanks to its formulation, the adhesive is suitable for bonding metals and for structural applications subjected to both static and dynamic loads. The main technical specifications of the adhesive and substrates used are reported in Table 1.

Table 1. Mechanical properties of 6061-T6 aluminum substrates and main characteristics of the 3M™ EPX DP490 structural adhesive used for single-lap joints.

Substrate	AA6061-T6	Adhesive	3M™ DP490
Density [g/cm^3]	2.70	Chemical composition	Epoxy
Tensile strength [MPa]	327.1±0.48	Mix ratio	2:1
Yield strength [MPa]	273.3±4.21	Work life @ 23°C	1.5 h
Elastic modulus [GPa]	36.09±1.95	Handling time @ 23°C	4÷6 h
Elongation at break [%]	18.6±0.3	Full strength time @ 23°C	7 days

Surface preparation methods.

Substrates underwent different surface preparation protocols for comparison. The first consists of degreasing (DG) with acetone-soaked absorbent paper for the reference condition samples. The second is mechanical abrasion (AB) using a Scotch-Brite™ 7447 PRO pad, which is the standard industrial pretreatment. The third is an alternative laser texturing treatment (TXT).

Particular attention is given to the role of laser-induced surface features (LIPSS) in promoting adhesion. The laser employed is a picosecond Ekspla Atlantic 50, ≈with a pulse duration of about 10 ps. The wavelength used is 1064 nm. The repetition rate is set at 333 kHz as a compromise between speed and pulse overlapping. The system includes a Raylase Superscan V galvanometric scanning head to ensure precise beam trajectory control, while an F-theta lens provides a focused spot size of roughly 10 µm at the $1/e^2$ intensity. The chosen scanning strategy is parallel lines, 4.5 µm spaced, scanned at 1200 mm/s to have a homogeneous treated area, having the same energy deposition between and along the scanlines. The power was set at 0.3 W to have regular and clean LIPSS. This strategy was chosen for two main reasons: to increase the hydrophilicity of the base material, primarily through chemical oxidation [32], and to do this with a sufficient areal throughput. The process is carried out in an area of 16x28 mm, to ensure that the gluing area is covered, which is then suitably masked.

Twenty aluminum sheets were textured, for a total of five pairs per two conditions to be tested (bonding with and without the debonding method). For clarity, the entire methodology is summarized in Fig. 1, which explains the bonding and debonding/rebonding phases and where laser texturing and cleaning come into play. In this preliminary study, after cleaning, surface preparation was performed, followed by bonding without debonding methods. Bonding can then be performed using debonding methods to evaluate recyclability over multiple cycles.

Before bonding, all adherends were degreased to remove treatment residues and dirt, taking care that after laser treatment, the samples were only dried with hot air to avoid damaging the microstructure with mechanical actions.

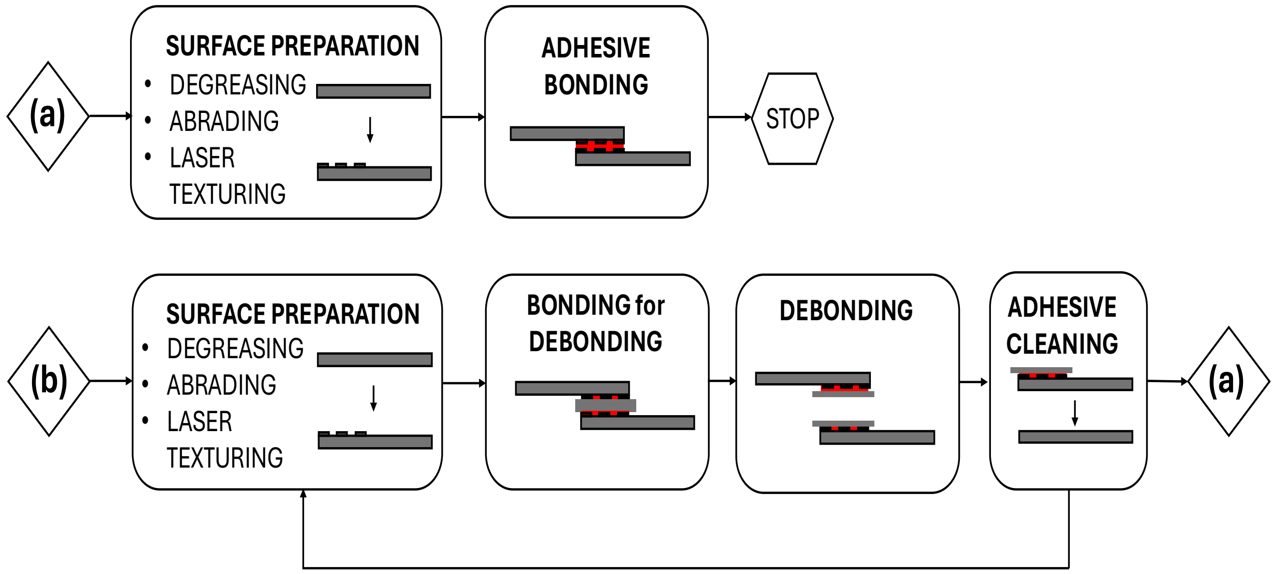

Fig. 1. Methodology of the work: a) laser texturing for the bonding process, b) laser texturing and cleaning for the rebonding process.

Single-lap joint manufacturing and debonding method used.

The bonding area was defined by using masking tape to ensure consistent overlap geometry. The adhesive was dispensed using a manual applicator equipped with a 2:1 ratio plunger and static mixer to ensure proper resin-hardener mixing. After assembly, the joints were subjected to uniform pressure to eliminate excess adhesive and to shape the fillet, minimizing stress concentrations at the edges. The specimens were then cured at room temperature for 24 hours, followed by a post-curing cycle at 80°C for 1 hour, as recommended by the adhesive manufacturer.

An electrothermal debonding technique was developed and evaluated using a metal mesh (MM) embedded within the adhesive layer of single-lap joints. The mesh served as a conductive element to locally heat the joint via the Joule effect, facilitating adhesive degradation and enabling manual disassembly.

The mesh is a woven stainless steel 304 fabric with a wire diameter of 0.05 mm and an aperture of 0.104 mm. It was cut to match the overlapping area and positioned between the aluminum alloy substrates during adhesive application.

Debonding was performed by connecting the mesh to a DC power supply (Kert Cosmo 3000), capable of delivering adjustable voltage and current. Preliminary trials were conducted to determine optimal electrical parameters. The final debonding protocol involved applying a voltage of 3.5–4.0 V and a current of 10 A for 3 minutes, resulting in a surface temperature of approximately 130°C, measured by a thermocouple. This condition was sufficient to soften the adhesive without exceeding the thermal limits of the substrate. Following treatment, the joints could be manually disassembled without tools, but the mechanical strength was reassessed via lap shear testing.

Laser Cleaning and surface preparation after debonding.

The methodology comprises the ablation of the thermosetting epoxy resin, while leaving a surface treatment on the aluminum.

The adopted strategy derives from preliminary investigations aimed at identifying the most effective approach for removing the adhesive without damaging the aluminum substrate. Two methods were initially considered: direct and selective ablation of the resin, and detachment by targeting the Al–Al-adhesive interface. Tests performed at 355 nm and 1064 nm revealed that UV radiation rapidly attacked aluminum, while near-IR provided better control over resin removal, despite its limited transparency through the adhesive. At high energy, both wavelengths ablated the resin. Considering material response and process efficiency, the definitive choice was 1064 nm, which offered higher power and energy per pulse, enabling faster and more productive cleaning.

The scanning strategy is a homogeneous treatment, with 400 kHz of repetition rate, scanning 4 µm spaced parallel lines at 2000 mm/s. Power is set at 1.42 W, and the number of passes changes depending on the adhesive thickness, from 20 to 30. The cleaning is carried out on an area of 16x28 mm. The process is carried out by keeping two dust-suction systems active to aspirate the particulate and fumes generated. Thirty aluminum sheets were cleaned, for a total of fifteen pairs, for three tested conditions (degreased, abraded, and textured after debonding).

Surface morphology and wettability characterization.

A VHX Keyence digital microscope equipped with two optical objectives (100-500x and 500-2500x) was used to obtain the morphology of the treated samples compared to the untreated and standard ones. The instrument with the supplied optics has a resolution of 0.1 µm, which covers the dimension expected from the LIPSS of the I harmonic.

Sample measurements of roughness were also taken using the Talyscan 150 profilometer to get a quick idea of the topography of the untreated material, treated with different surface preparation methods, then with laser cleaning and subsequent surface preparation methods. The instrument operates using triangulation laser technology. The area to be analysed was scanned with a spacing of 5 µm, and the measured data were processed using the dedicated TalyMap software. In the case of the first surface pretreatment, the area analyzed was 5x5 mm as it was visibly uniform. In the case of laser cleaning and subsequent preparation methods, the area analyzed was extended to 12.5x25 mm to account for all irregularities. The measure is based on an average of three different samples for each condition.

To validate the choice of texture evaluated in this study, wettability was measured using inks with known surface tension. The procedure involved applying the solution with the greatest surface tension onto the sample's surface. If the liquid spreads as a continuous film, the sample surface tension is at least equal to that of the applied solution. Conversely, if the liquid contracts and forms droplets, the sample has a lower surface tension, and a subsequent test using a solution with reduced surface tension is required. The solutions used for surface tension assessment were supplied by Plasmatreat GmbH in accordance with DIN 53914/ISO 304:1985 standards. Ethanol-based test inks (C Series) were employed, covering a surface tension range of 28–72 mN/m (surface tension of water) in 2 mN/m increments. Since the untreated material appears anisotropic due to the rolling process from which it is obtained, the wettability was evaluated both parallel and perpendicular respect the rolling direction.

Shear strength and bonding performance validation.

Lap shear tests were performed using an Instron 8802 universal testing machine, and the testing protocol was defined within the Bluehill software. The specimens were loaded at a constant displacement rate of 1.3 mm/min. To ensure pure shear loading, spacers matching the specimen's thickness were placed in the grips to prevent bending in the overlap region.

Lap shear tests were performed on pretreated and untreated samples, on samples prepared for detachment without applying voltage to degrade the joint, and on samples prepared for detachment but after electrothermal degradation, to quantify the effects on mechanical strength.

Results and Discussion

Surface preparation morphological results.

The morphology of the degreased (a), abraded (b), and textured (c) samples is shown
Fig. 2, in which the signs of lamination of the as-is sample, the random scratches of abrasion, and the uniformity of the laser treatment are clearly visible all over the surface. The sample roughness values for the different treatments are shown in Table 2. As might be expected, mechanical abrasion slightly increases roughness values, while laser texturing, which leaves a micrometric texture, reduces them.

Table 2. Surface roughness values for the different surface pretreatments: Arithmetic mean height (Sa); Root mean square height (Sq); Maximum height (Sz); Skewness (Ssk); Kurtosis (Sku).

Surface pretreatment	Sa [μm]	Sq [μm]	Sz [μm]	Ssk [-]	Sku [-]
Degreased	3.88±0.30	5.06±0.42	53.3±5.39	-0.26±0.35	4.26±0.31
Abraded	5.08±0.33	6.45±0.47	52.4±5.19	0.21±0.19	3.28±0.19
Laser textured	2.11±0.38	2.64±0.48	20.1±2.48	0.05±0.09	2.96±0.01

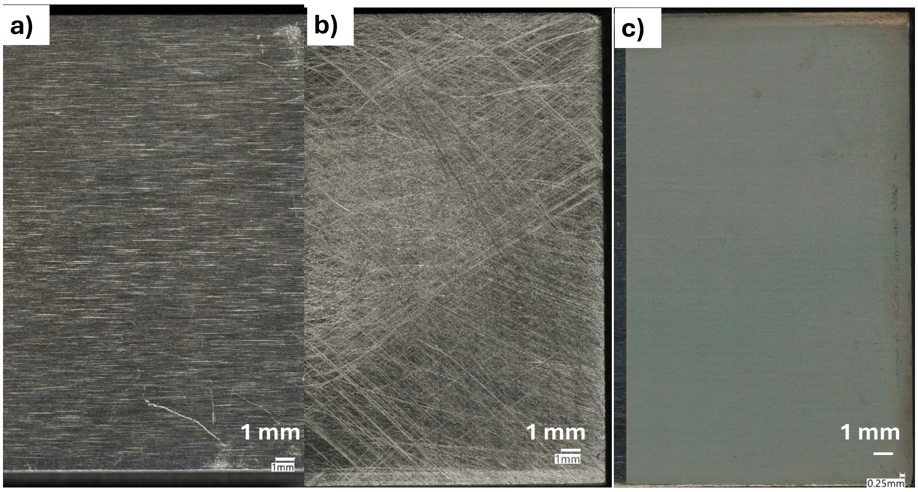

Fig. 2. Digital microscope images of the degreased (a), abraded (b), and textured (c) samples.

Fig. 3- b shows the periodic surface structures induced by the laser on the Aluminum substrate, at high magnification, in which the regularity of the structures and the size, equal to approximately 1 μm, can be appreciated. In the image, the structures appear almost vertical, perpendicular to the direction of pull, to offer maximum resistance to the shear force. At the macroscopic level, texturing overlaps with the structure of the untreated material, which is visible in Fig. 3-a.

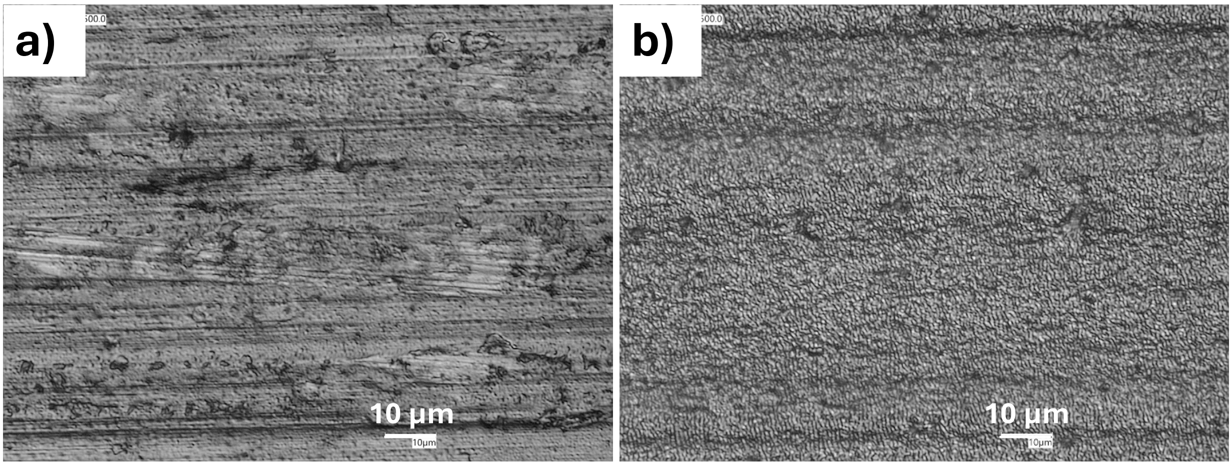

Fig. 3. Digital image of untreated (a) and LIPSS textured (b) Aluminum substrate at high magnification.

Wettability results.

A solution with a surface tension of the water was applied to both treated and untreated specimens. Measurements were repeated at least four times for each condition. The surface tension assessment was performed immediately after the laser treatment to capture its initial effect on wettability. After 24 and 48 hours, the results remained consistent. On all treated samples, the liquid spread uniformly, forming a continuous film, which indicates hydrophilic behavior, see Fig. 4-b.

In contrast, on untreated samples, the liquid retracted into droplets. Additional tests using solutions with progressively lower surface tension values were carried out on the untreated substrates, revealing that their surface tension was below 46 mN/m in the rolling direction and below 44 mN/m in the perpendicular direction. An example of this can be seen in Fig. 4-a. Indeed, the choice of texture for the proposed objective is validated.

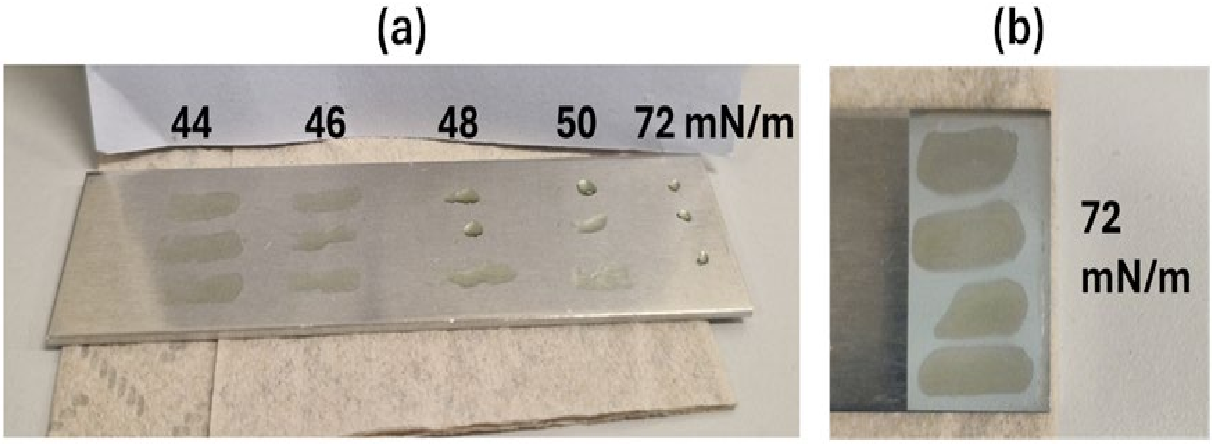

Fig. 4. Surface tension evaluation of the a) untreated and b) laser-treated sample.

Bonding mechanical tensile test results and fracture surface analysis.

The results of tensile tests on bonded joints are visible in
Fig. **5**. Laser treatment can increase the mechanical strength to 157% respect to the degreased bonded joint, while also increasing the displacement value at break. This leads to an increase in absorbed energy of more than three times compared to degreased material and more than double compared to abraded material. The results also demonstrate that the insertion of the metal mesh as a debonding method does not significantly affect the strength of the joint, which becomes around 93% for the textured sample, 95% for the abraded, and 84% for the degreased.
Furthermore, the fracture surfaces analysis in Fig. 6 shows that the de-adhesive failure occurred on the degreased samples, becomes mixed for the abraded sample, and is completely cohesive for the textured sample. This demonstrates greater adhesion between the substrate and adhesive surfaces. Laser texturing treatment uniformly modifies both the chemistry and the morphology of the surface, improving mechanical interlocking.

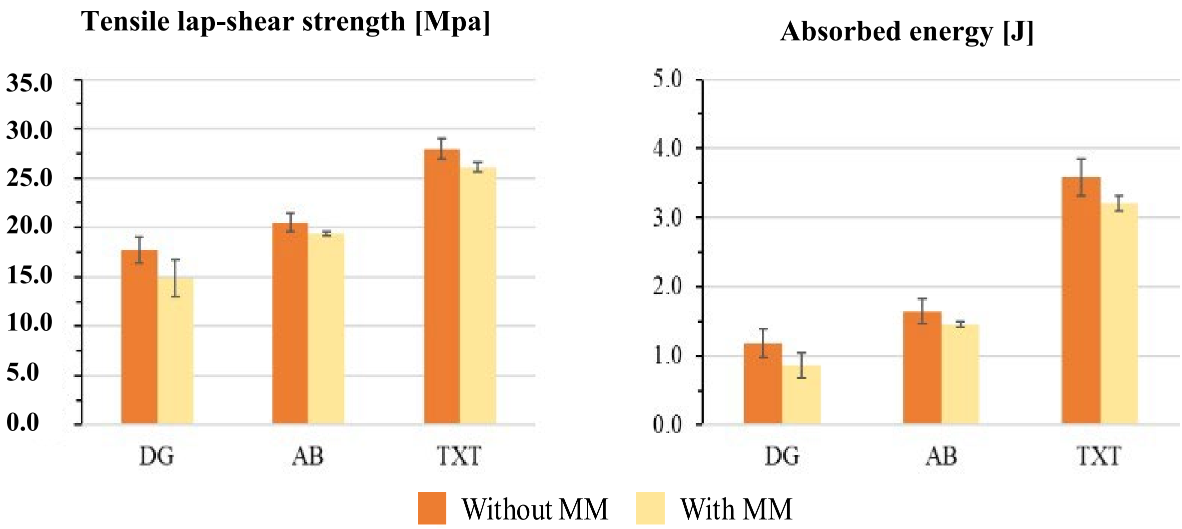

Fig. 5. Tensile test results on bonded joints without and with the metal mesh (MM).

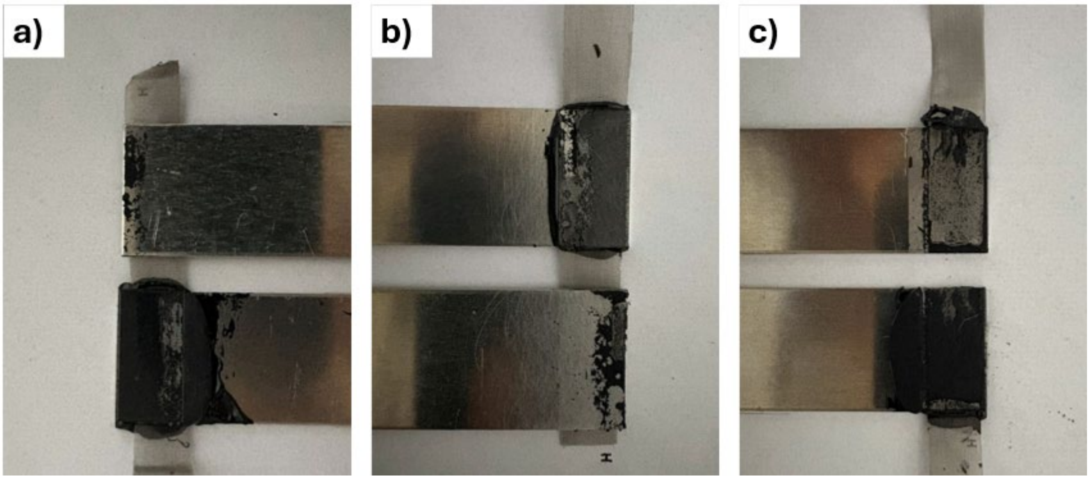

Fig. 6. Fracture surfaces analysis of the a) degreased, b) abraded, c) textured bonded joints.

Cleaning morphological and wettability results.

The joints subjected to debonding were laser cleaned for the subsequent rebonding. An example of the cleaning process effect is shown in Fig. 7, which depicts the two textured adherends separated after the mechanical test, with the adhesive on both surfaces (a, c) and after cleaning (b, d). The sample roughness values for the different treatments after laser cleaning are shown in Table 3. In the case of post-laser cleaning treatments, roughness increases due to some localized adhesive residues remaining on the surface, visible as small dots highlighted by the white arrows in Fig. 7 -b and d.

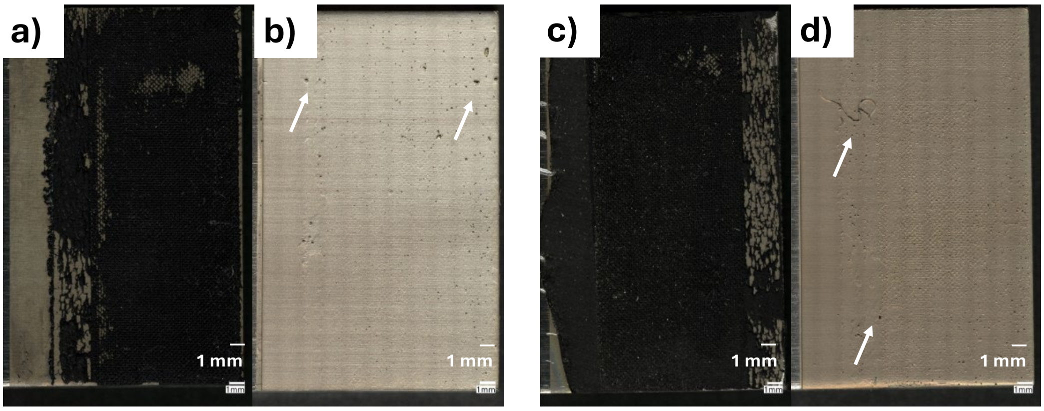

Fig. 7. Cleaning surfaces on debonded samples: example of textured: the two adherends before (a, c) and after laser cleaning (b, d): white arrows indicate localized adhesive residues.

Table 3. Surface roughness values for the different surface pretreatments after laser cleaning.

Surface pretreatment	Sa [µm]	Sq [µm]	Sz [µm]	Ssk [-]	Sku [-]
Degreased	4.96±1.39	9.66±2.15	199.9±86.5	6.90±4.00	107.8±89.8
Abraded	8.80±4.45	15.5±7.83	182.8±68.1	1.49±1.97	24.9±8.23
Laser textured	14.2±9.93	34.3±22.2	552.6±319.2	7.64±2.04	96.1±48.9

Laser-cleaned surfaces were then re-prepared according to the original three procedures before the rebonding process: degreasing, abrasion, and texturing. It is worth analyzing in detail how the texturing appears on the cleaned material: cleaning creates an uneven surface, visible in Fig. 8-a, with micrometric roughness, in some places there are LIPSS, but they are quite irregular. The subsequent LIPSS texturing adapts to the rough substrate and becomes more regular, see Fig. 8-b. Furthermore, wettability confirms that surface energy is constantly above 72 mN/m for post-cleaning texture.

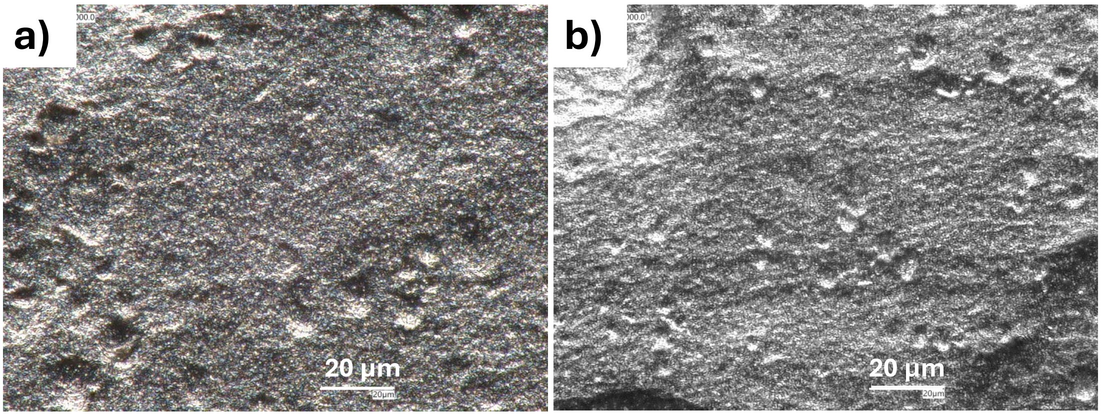

Fig. 8. Digital image of laser cleaned (a) and LIPSS texturing after cleaning (b) at high magnification.

Rebonding mechanical tensile test results and fracture surface analysis.

The mechanical results of the bonded, debonded, and rebonded joints after cleaning are compared in Fig. 9. Shear tests on the cleaned and rebonded joints show that the surface condition left by laser cleaning increases the mechanical strength of the degreased rebonded joint up to 178% and to 103% compared to the previously textured one. Therefore, surface improvement over the original degreased surfaces can be achieved with the cleaning treatment itself. Only the rebonding of the cleaned and abraded surfaces shows, on average, a slight decrease to 97%, a value that remain inside the standard deviation. Subsequent abrasion does not further improve resistance but restores the original surface. On the other hand, combining these methods would not be advantageous from an industrial point of view, because once the surface has been cleaned with the laser, better results can be achieved (see rebonding results on the degreased surfaces). It is presented for comparison purposes.

In addition, the fracture surfaces in Fig. 10 show that laser cleaning produces a cohesive fracture for both degreased and textured samples, while abrasion again shows a mixed fracture.

When testing the mechanical strength of joints subjected to debonding, shear strength is reduced by 7.20% for textured, 5.42% for abraded, and 4.58% for degreased, respect to the bonded one. The lowest resistance of the degreased allowed separation even manually.

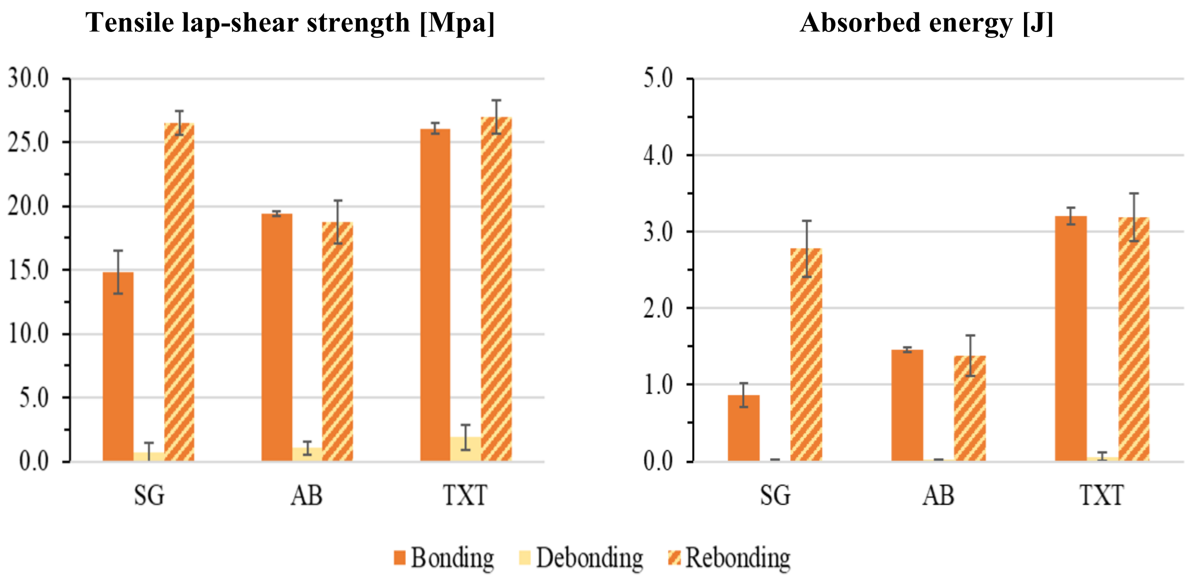

Fig. 9. Comparison between tensile test results: bonded, debonded, and rebonded joints.

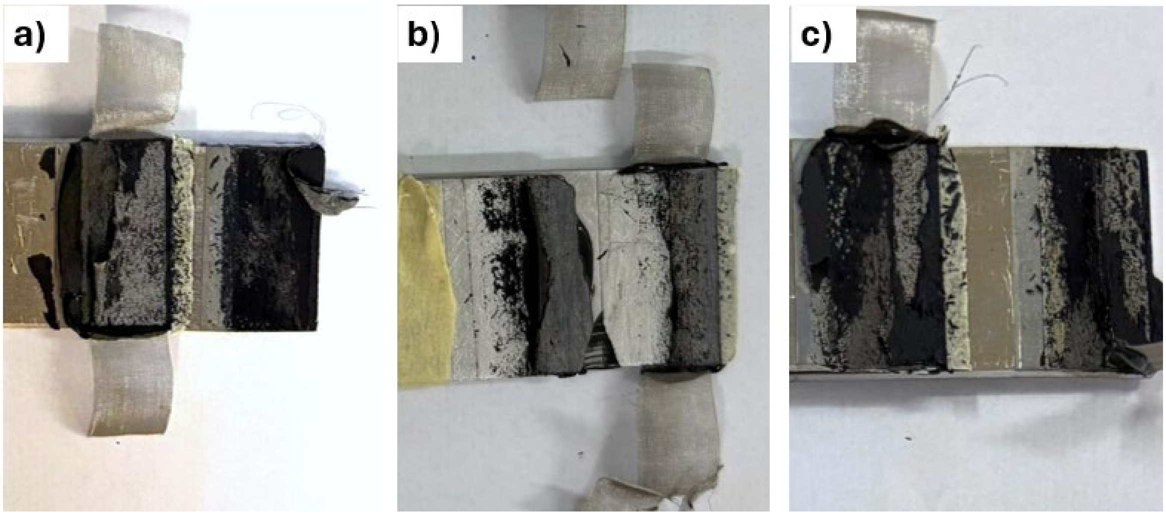

Fig. 10. Fracture surfaces analysis of the a) degreased, b) abraded, c) textured rebonded joints.

Conclusion

The growing demand for sustainable manufacturing and circular economy practices calls for innovative solutions to overcome the limitations of permanent adhesive joints, which hinder component reuse and increase waste. This work explored laser cleaning and texturing as strategies to enable the reuse of single-lap adhesive-bonded joints, addressing the challenge of recyclability in structural bonding. The study showed that controlled debonding using a metal mesh embedded in the adhesive promotes the separation of the joint once it has been disused, preserving the strength of the original joint during operation and preventing post-debonding deformation. Subsequent laser cleaning effectively removes the residual adhesive and not only restores the substrate, but also introduces micrometric roughness, enhancing adhesion performance.

Initial bonding tests confirmed that laser texturing significantly improves the shear strength (up to 1.5 times) and energy absorption (up to 3 times) compared to degreasing and abraded conventional surface preparation (1.36 times and 2 times, respectively).

After debonding, laser cleaning alone proved sufficient to recover surface properties and even increase the strength of rebonded joints beyond their original degreased condition. While additional abrasion after cleaning offered no further benefit, the results highlight the potential of laser-based treatments to simplify and optimize the rebonding process.

These findings demonstrate that laser cleaning can be effectively integrated into circular manufacturing strategies, as the process not only enables surface preparation for rebonding but also enhances joint strength. This study primarily aimed to validate the overall methodology, acknowledging that cleaning parameters can be further optimized using different laser sources.

The concept was initially validated through preliminary tests on 6016 aluminum alloy; however, due to its inherently low baseline strength, the research ultimately focused on 6061 aluminum alloy. Given that the method relies on controlled surface-morphological modification, it is reasonable to expect that it can be extended to other structural materials and a wide range of adhesive systems. Laser ablation is already known for its versatility in processing complex materials, with no significant inherent limitations.

Future research should investigate the feasibility of multiple bonding cycles without compromising the substrate's mechanical integrity. Since laser treatment typically affects only a few micrometers of the surface, we are confident that several successive bonding cycles are achievable. This approach also shows promise for industrial-scale adoption, provided that process parameters are optimized for the different phases, and that economic assessments could confirm the advantages of closed-loop recycling systems aimed at reducing waste and extending component lifetimes.

From an industrial perspective, laser cleaning is both economically and environmentally sustainable over the long term, despite higher initial equipment costs compared to conventional techniques. Its advantages stem from the absence of consumables (e.g., abrasives, chemical agents), low energy demand, and reduced waste-management requirements. When combined with laser texturing, which further enhances material performance while retaining similar sustainability benefits, the approach becomes even more effective. Successful integration requires precise control of laser power and parameters such as pulse duration and frequency. Modern pulsed fiber lasers allow seamless switching between cleaning and texturing modes by adjusting the software settings alone.

References

[1] E. Georgantzia, M. Gkantou, G.S. Kamaris, Aluminium alloys as structural material: A review of research, Engineering Structures 227 (2021) 111372. https://doi.org/10.1016/j.engstruct.2020.111372.

[2] Y. Sun, The use of aluminum alloys in structures: Review and outlook, Structures 57 (2023) 105290. https://doi.org/10.1016/j.istruc.2023.105290.

[3] K. Martinsen, S.J. Hu, B.E. Carlson, Joining of dissimilar materials, CIRP Annals 64 (2015) 679–699. https://doi.org/10.1016/j.cirp.2015.05.006.

[4] Handbook of adhesives: edited by Irving Skeist. 683 pages, diagrams, illustrations, 612 × 10 in. New York, Reinhold Publishing Corp., 1962. Price, $23.50., Journal of the Franklin Institute 274 (1962) 324. https://doi.org/10.1016/0016-0032(62)90851-7.

[5] U. Tiringer, J. Kovač, I. Milošev, Effects of mechanical and chemical pre-treatments on the morphology and composition of surfaces of aluminium alloys 7075-T6 and 2024-T3, Corrosion Science 119 (2017) 46–59. https://doi.org/10.1016/j.corsci.2017.02.018.

[6] J. Li, Y. Li, M. Huang, Y. Xiang, Y. Liao, Improvement of aluminum lithium alloy adhesion performance based on sandblasting techniques, International Journal of Adhesion and Adhesives 84 (2018) 307–316. https://doi.org/10.1016/j.ijadhadh.2018.04.007.

[7] J. Min, H. Wan, B.E. Carlson, J. Lin, C. Sun, Application of laser ablation in adhesive bonding of metallic materials: A review, Optics & Laser Technology 128 (2020) 106188. https://doi.org/10.1016/j.optlastec.2020.106188.

[8] D. Morello, C. Leone, G. Lamanna, G. Silvio, A two-step full laser surface treatment to improve the adhesive bonding of aluminium-aluminium joints, International Journal of Adhesion and Adhesives 142 (2025) 104089. https://doi.org/10.1016/j.ijadhadh.2025.104089.

[9] G.W. Critchlow, D.M. Brewis, Review of surface pretreatments for aluminium alloys, International Journal of Adhesion and Adhesives 16 (1996) 255–275. https://doi.org/10.1016/S0143-7496(96)00014-0.

[10] Review on Adhesives and Surface Treatments for Structural Applications: Recent Developments on Sustainability and Implementation for Metal and Composite Substrates, (n.d.). https://www.mdpi.com/1996-1944/13/24/5590 (accessed October 22, 2025).

[11] N. Naat, Y. Boutar, S. Naïmi, S. Mezlini, L.F.M. Da Silva, Effect of surface texture on the mechanical performance of bonded joints: a review, The Journal of Adhesion 99 (2023) 166–258. https://doi.org/10.1080/00218464.2021.2008370.

[12] X. Zou, L. Liu, T. Chen, L. Wu, K. Chen, L. Kong, M. Wang, Laser surface treatment to enhance the adhesive bonding between steel and CFRP: Effect of laser spot overlapping and pulse fluence, Optics & Laser Technology 159 (2023) 109002. https://doi.org/10.1016/j.optlastec.2022.109002.

[13] Z. Feng, H. Zhao, C. Tan, B. Zhu, F. Xia, Q. Wang, B. Chen, X. Song, Effect of laser texturing on the surface characteristics and bonding property of 30CrMnSiA steel adhesive joints, Journal of Manufacturing Processes 47 (2019) 219–228. https://doi.org/10.1016/j.jmapro.2019.09.046.

[14] A. Ragusich, G. Taillon, M. Meunier, L. Martinu, J.E. Klemberg-Sapieha, Selective pulsed laser stripping of TiAlN erosion-resistant coatings: Effect of wavelength and pulse duration, Surface and Coatings Technology 232 (2013) 758–766. https://doi.org/10.1016/j.surfcoat.2013.06.092.

[15] J. Gu, X. Su, W. Li, M. Xin, D. Zhang, Y. Jin, J. Xu, B. Guo, Investigation on laser paint stripping of CFRP: Morphological evolution, damage mechanism, and adhesive performance, Journal of Materials Research and Technology 31 (2024) 3690–3702. https://doi.org/10.1016/j.jmrt.2024.07.063.

[16] L. Hou, F. Yin, S. Wang, J. Sun, H. Yin, A review of thermal effects and substrate damage control in laser cleaning, Optics & Laser Technology 174 (2024) 110613. https://doi.org/10.1016/j.optlastec.2024.110613.

[17] S. Genna, C. Leone, E. Mingione, Surface cleaning of 34CrMo4 steel pipes by using pulsed fibre laser, Int J Adv Manuf Technol 125 (2023) 231–244. https://doi.org/10.1007/s00170-022-10648-8.

[18] V. Siciliani, Effect of surface preparation on adhesive bonding of CFRP compression molding laminates, in: 2025: pp. 2193–2202. https://doi.org/10.21741/9781644903599-236.

[19] V. Siciliani, R. Pelaccia, D. Castagnetti, L. Raimondi, L. Donati, L. Orazi, M. Alfano, Enhancing the shear strength of adhesive bonded compression-molded CFRP laminates using selective UV picosecond laser treatment, Int J Adv Manuf Technol 141 (2025) 5697–5708. https://doi.org/10.1007/s00170-025-16985-8.

[20] V. Narayanan, R. Singh, D. Marla, Optimization of Nanosecond Pulsed Laser Cleaning of Rust, Lasers Manuf. Mater. Process. 12 (2025) 68–85. https://doi.org/10.1007/s40516-025-00282-z.

[21] M.P. Mateo, G. Nicolas, V. Piñon, A. Ramil, A. Yañez, Laser cleaning: an alternative method for removing oil-spill fuel residues, Applied Surface Science 247 (2005) 333–339. https://doi.org/10.1016/j.apsusc.2005.01.086.

[22] J. Gacs, E. Sára Bogya, L. Kocsis, T. Jacob, Application of laser cleaning on AlMg4.5Mn0.4 sheets for adhesive bonding, International Journal of Adhesion and Adhesives 115 (2022) 103132. https://doi.org/10.1016/j.ijadhadh.2022.103132.

[23] T. Shi, C. Wang, G. Mi, F. Yan, A study of microstructure and mechanical properties of aluminum alloy using laser cleaning, Journal of Manufacturing Processes 42 (2019) 60–66. https://doi.org/10.1016/j.jmapro.2019.04.015.

[24] G. Zhu, Z. Xu, Y. Jin, X. Chen, L. Yang, J. Xu, D. Shan, Y. Chen, B. Guo, Mechanism and application of laser cleaning: A review, Optics and Lasers in Engineering 157 (2022) 107130. https://doi.org/10.1016/j.optlaseng.2022.107130.

[25] A. Wang, A. Feng, X. Gu, X. Pan, J. Yu, Z. Jiang, Effect of picosecond laser cleaning on surface morphology and properties of stainless steel, Optics & Laser Technology 159 (2023) 109041. https://doi.org/10.1016/j.optlastec.2022.109041.

[26] C. Zhang, Y. Zhang, L. Chen, Y. Chen, Effect of laser micromachining crater-array–multi-grooves on the bonding strength and failure mode of aluminum alloy adhesive joints, Optics & Laser Technology 175 (2024) 110803. https://doi.org/10.1016/j.optlastec.2024.110803.

[27] C. Mandolfino, E. Lertora, S. Genna, C. Leone, C. Gambaro, Effect of Laser and Plasma Surface Cleaning on Mechanical Properties of Adhesive Bonded Joints, Procedia CIRP 33 (2015) 458–463. https://doi.org/10.1016/j.procir.2015.06.054.

[28] C. Leone, A. Paoletti, P. Babu Yanala, F. Lambiase, Improving bonding strength of aluminium-PEEK hybrid metal-polymer joints by two-step laser surface treatment, Optics & Laser Technology 170 (2024) 110304. https://doi.org/10.1016/j.optlastec.2023.110304.

[29] L. Romoli, F. Moroni, M.M.A. Khan, A study on the influence of surface laser texturing on the adhesive strength of bonded joints in aluminium alloys, CIRP Annals 66 (2017) 237–240. https://doi.org/10.1016/j.cirp.2017.04.123.

[30] F. Moroni, F. Musiari, A. Pirondi, Influence of laser ablation-induced surface topology on the mechanical behaviour of aluminium bonded joints, Proceedings of the Institution of Mechanical Engineers, Part L: Journal of Materials: Design and Applications 233 (2019) 505–520. https://doi.org/10.1177/1464420718813388.

[31] Standard Test Method for Apparent Shear Strength of Single-Lap-Joint Adhesively Bonded Metal Specimens by Tension Loading (Metal-to-Metal), (n.d.). https://store.astm.org/d1002-10r19.html (accessed November 6, 2025).

[32] C. Berrospe-Rodriguez, B. Baskar, J. Williams, G. Aguilar, Wettability tuning on stainless steel LIPSS by laser oxidation and its implication on cavitation bubble dynamics, Applied Surface Science 672 (2024) 160803. https://doi.org/10.1016/j.apsusc.2024.160803.